Supporting Information

Recyclable indole-based polymer for trinitrotoluene adsorption via synergistic effect of dipole-π and donor-acceptor interactions

Yan Wang,[ab] Lin Zhang,*[ab] Li Yang,*[ac] Yuanchi Ma,[c] Guanjun Chang*[ac]

[a] State Key Laboratory of Environment-friendly Energy Materials & School of Material Science and Engineering, Southwest University of Science and Technology, Mianyang 621010, P. R. China.

[b] Science and Technology on Plasma Physics Laboratory, Research Center of Laser Fusion, China Academy of Engineering Physics, Mianyang 621900, P. R. China.

[c] Department of Chemical and Biomolecular Engineering, University of Pennsylvania, Philadelphia, Pennsylvania, 19104, United States.

Corresponding author: Prof. Lin Zhang, Email: zhlmy@sina.com;

Prof. Li Yang, Email: yanglichem628@126.com;

Prof. Guanjun Chang, Email: gjchang@mail.ustc.edu.cn.

Main materials and instruments

4-Aminoindole (4-AIN, 97%), indole (IN, 97%), Aniline (AR), 1,2-dichloroethane (AR), iron (III) chloride ($FeCl_3$, AR), formaldehyde dimethyl acetal (FDA, AR), methanol (AR), sulfuric acid (H_2SO_4, 98%), anhydrous sodium sulfite (Na_2SO_3, AR), sodium hydroxide (NaOH, AR), hydrochloric acid (HCl, 12 M) and acetone (AR) were purchased from Shanghai Reagent (Shanghai, China). TNT was obtained from the Department of Materials Science and Engineering of the Southwest University of Science and Technology, China.

UV/Vis absorption spectra were obtained on the UV-1800 spectrometer. Fourier transform infrared spectroscopy (FT-IR) analysis was conducted on the Nicolet-5700 FT-IR spectrometer with KBr pellet technique in the range of 4000-400 cm^{-1}. The ^{13}C CP/MAS NMR spectrum was conducted on a Bruker Avance III 400 NMR spectrometer. The elemental analysis was performed using a Vario EL III apparatus. The scanning electron microscopy (SEM) was curried on an Ultra 55 microscope system. The pH values were precisely determined by using a pH-meter (pHS-$3C^+$). The N_2 adsorption-desorption isotherms were measured on the Quantachrome automated adsorption analyzer at 77.3 K.

Preparation and characterizations of PIN and PAB

PIN: IN (0.234 g, 2 mmol) was added to anhydrous 1,2-dichloroethane (20 mL) under a flow of argon, followed by FDA (0.3044 g, 4 mmol). $FeCl_3$ (0.650 g, 4 mmol) was added and the reaction heated to 80 °C for 18 h (Scheme S1). The solid product was collected by filtration and washed with methanol and HCl (10%) until the filtrate

liquor was nearly colorless to completely remove the unreacted Fe(III) and starting precursor. The product was further washed with deionized water until the filtrate liquor was neutral. The final product was further purified by soxhlet extraction in methanol for 24 h, and dried by CO_2 supercritical drying.

PAB: Aniline (0.186 g, 2 mmol) was added to anhydrous 1,2-dichloroethane (20 mL) under a flow of argon, followed by FDA (0.3044 g, 4 mmol). $FeCl_3$ (0.650 g, 4 mmol) was added and the reaction heated to 80 °C for 18 h (Scheme S3). The solid product was collected by filtration and washed with methanol and HCl (10%) until the filtrate liquor was nearly colorless to completely remove the unreacted Fe(III) and starting precursor. The product was further washed with deionized water until the filtrate liquor was neutral. The final product was further purified by soxhlet extraction in methanol for 24 h, and dried by CO_2 supercritical drying.

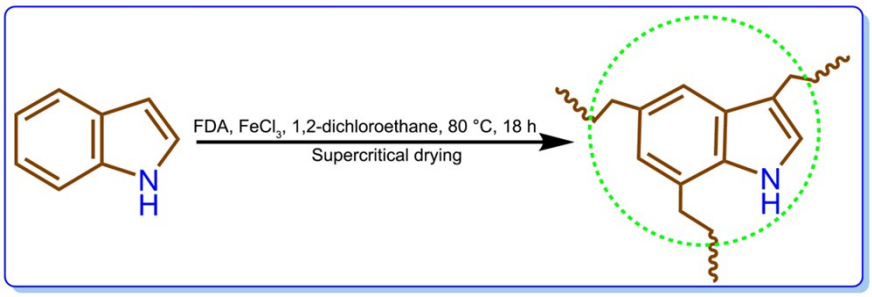

Scheme S1 Synthetic route of PIN.

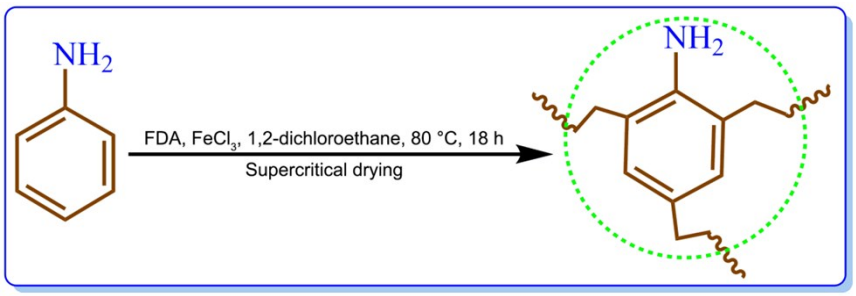

Scheme S2 Synthetic route of PAB.

In the FT-IR spectrum of PAIN (Fig. S1A), the peak at 3404.5 cm^{-1} was attributed to the stretching vibrations of N-H in primary amine and indole amine. The peaks at 2929.0 cm^{-1} and 2966.3 cm^{-1} were assigned to the stretching vibration of -CH_2- in the polymer network and the peaks at 1626.6 cm^{-1} and 1452.8 cm^{-1} corresponded to the vibrations of the aromatic ring skeleton. The peaks in ^{13}C CP/MAS NMR spectrum at 169-103 ppm were ascribed to the indole group carbons, and the signals located at 35-40 ppm were assigned to the methylene carbons (Fig. S1B).

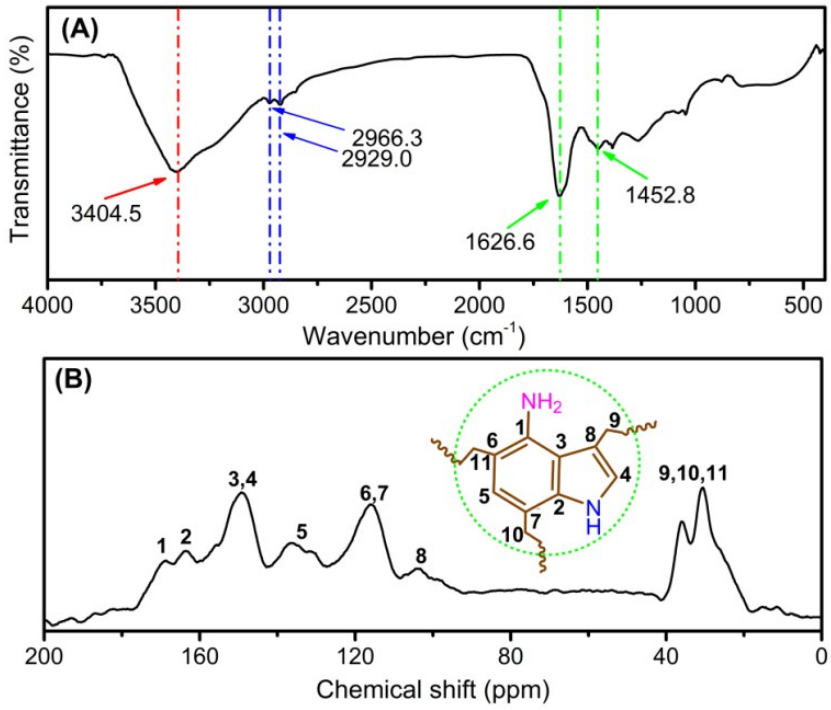

Fig. S1 (A) FT-IR spectrum and (B) ^{13}C CP/MAS NMR spectrum of PAIN.

PIN and PAB were characterized by FT-IR, and the results were in good agreement with the proposed structures (Fig. S2 and S3). In order to further understand the structures of the resulting materials, the element analysis was also investigated, and the results were listed in Table S1. PAIN: Yield: 95%; Anal. Calcd for $C_{11}H_{11}N_2$: C, 77.2; H, 6.4; N, 16.4; Found: C, 74.8; H, 4.8; N, 14.3. PIN: Yield: 90%; Anal. Calcd

for $C_{11}H_{10}N$: C, 84.6; H, 6.4; N, 8.9; Found: C, 82.5; H, 5.6; N, 7.8. PAB: Yield: 95%; Anal. Calcd for $C_9H_{10}N$: C, 81.8; H, 7.6; N, 10.6; Found: C, 84.3; H, 9.0; N, 6.3. Deviations for the expected values were expected for such polymers due to incomplete combustion and trapped adsorbates including gases and water vapor.

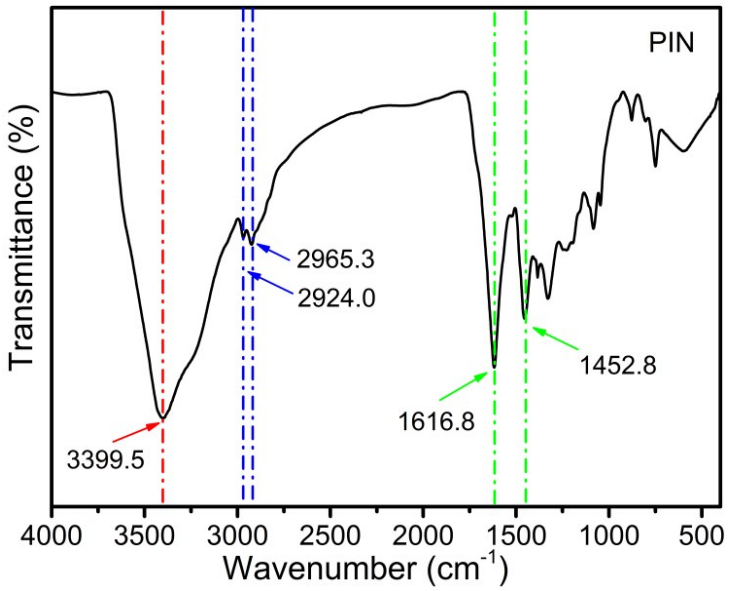

Fig. S2 FT-IR spectrum of PIN.

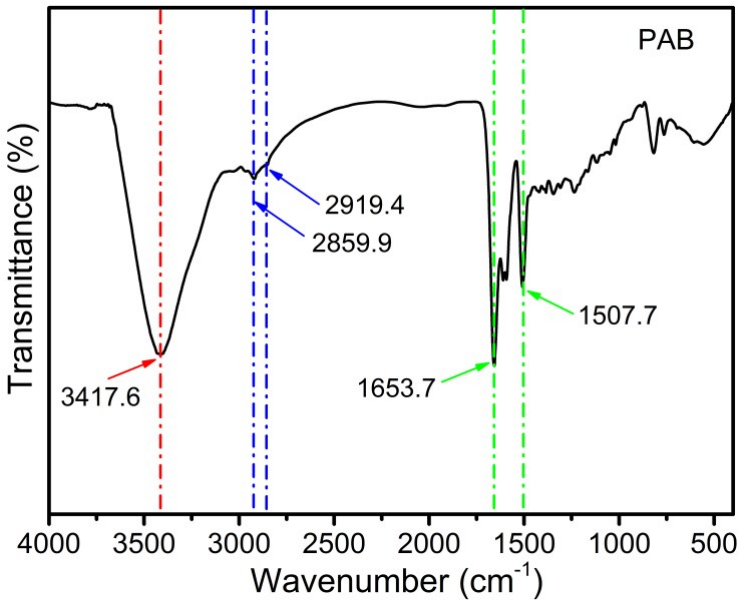

Fig. S3 FT-IR spectrum of PAB.

Table S1 Elemental analysis for PAIN, PIN and PAB.

Sample	Expected % C	Found % H	Expected % N	Found % N	Expected % H	Found % H
PAIN	77.2	6.4	16.4	74.8	4.8	14.3
PIN	84.6	6.4	8.9	82.5	5.6	7.8
PAB	81.8	7.6	10.6	84.3	9.0	6.3

Porosities of the PIN and PAB

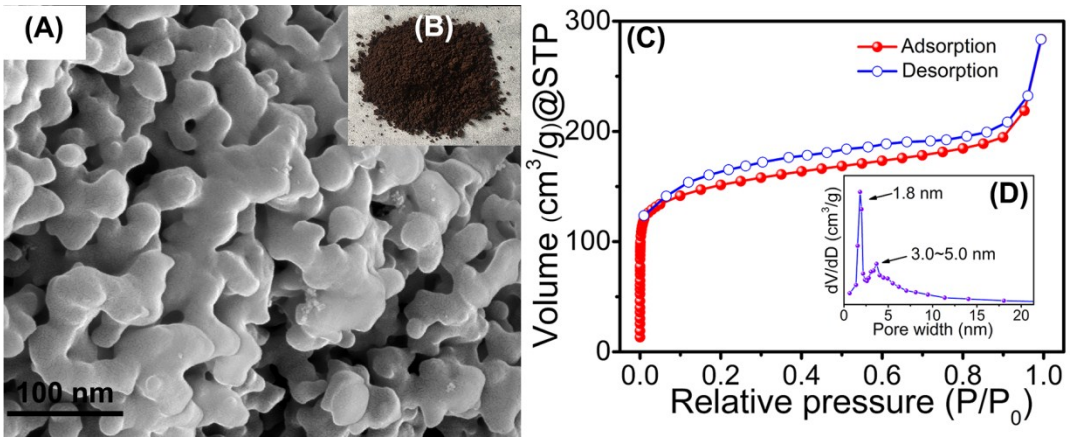

Fig. S4 SEM image; (B) Photograph; (C) N_2 adsorption-desorption isotherms and (D) pore size distribution of PIN.

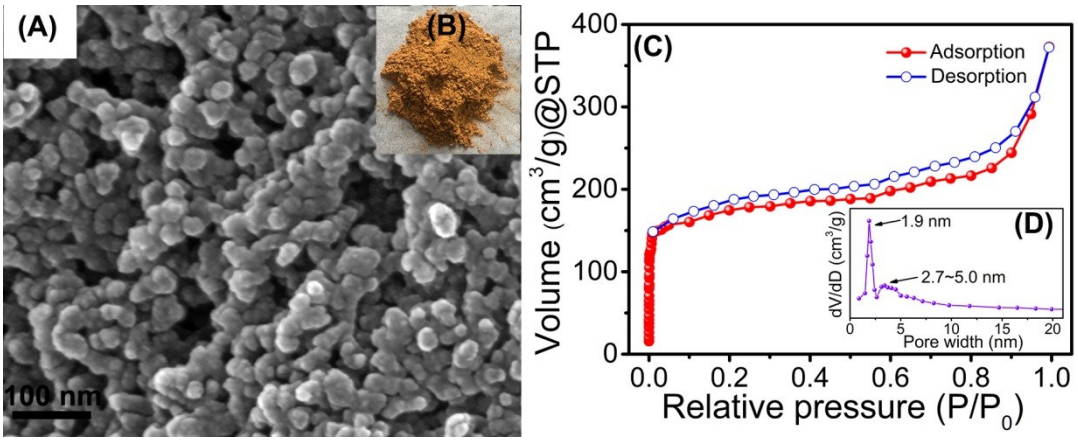

Fig. S5 (A) SEM image; (B) Photograph; (C) N_2 adsorption-desorption isotherms and (D) pore size distribution of PAB.

Determination of TNT concentration

TNT concentrations were determined by Na_2SO_3 titration method.[1] TNT solution (0.5 mL) with different concentrations (0, 1.25, 2.50, 3.75, 5.00, 6.25 and 7.50 mg L^{-1}, respectively), H_2SO_4 (3.00 mL, 5.4 M) and Na_2SO_3 solutions (5.00 mL, 200 g L^{-1}) were successively added. The mixture solutions were diluted to 20 mL with deionized water. After 15 min, the UV/Vis absorption spectra were measured. The relationship between absorbance (A) at 415 nm and TNT standard concentration was drawn in Fig. S6A. The calibration curve for A value against TNT concentration was linear in the range from 0 to 7.50 mg L^{-1} and fitted the linear equation A=0.00439+0.03689 c_{TNT} (c_{TNT} represents the concentration of TNT in *mg* L^{-1}) (Fig. S6B). The residual TNT concentration was calculated according to the standard curve in this study.

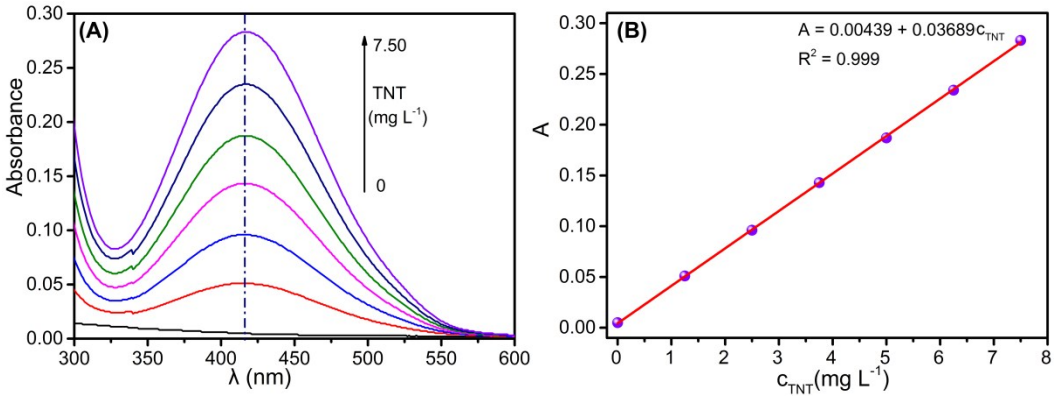

Fig. S6 (A) Absorbance spectra of standard TNT solutions with different concentrations. (B) Linear relationship between A and TNT concentrations.

Procedure for TNT adsorption

To investigate the effect of pH, the pH of initial TNT aqueous solution (200 mg L^{-1}) was adjusted by HCl (0.1 M) and NaOH (0.1 M) ranging from 2 to 11. Adsorption kinetic experiment was performed by mixing PAIN (5 mg), TNT aqueous solution (5

mL, 200 mg L^{-1}), pH (7) followed by stirring at 298 K. Adsorption isotherm experiment was conducted at 298 K by adding PAIN (5 mg) into TNT aqueous solution (5 mL) with different concentrations (50, 75, 100, 125, 150, 175 and 200 mg L^{-1}) at pH 7 for 12 h. Then, the solid-liquid separation was achieved by centrifugation at 1000 rpm, the residual TNT concentrations were determined. The equilibrium concentration (c_e) was calculated referring to the calibration curve of TNT (Fig. S6B). The main factors for the adsorption of TNT including contact time, initial concentration of TNT, and pH value were discussed. The equilibrium adsorption capacity (q_e) was calculated as follows:

$$q_e(mg\ g^{-1}) = \frac{(c_i - c_e)V}{1000w} \quad (1)$$

Where c_i ($mg\ L^{-1}$) and c_e ($mg\ L^{-1}$) are the initial concentration and equilibrium concentration of TNT, respectively. V is the volume of the solution in mL and w is the weight of the adsorbent in g. For comparison, the adsorption of TNT by PIN and PAB were discussed in this study as the above methods.

Regeneration experiment

PAIN (50 mg) was dispersed in 100 mL glass bottle containing TNT aqueous solution (50 mL, 200 mg L^{-1}) as used in the adsorption procedure. Once equilibrium was achieved, the PAIN loaded with TNT were separated and placed in the 250 mL stoppered conical flask containing of acetone (150 mL) for desorption, and stirred at 300 rpm for 72 h. After separation and washing with deionized water, the solid was dried in a convection oven at 45 °C for 24 h. The regenerated PAIN was then employed in the next adsorption experiment. All the studies manifested above were

also conducted with acetone as eluent. The recovery (R) of q_e was defined as,

$$Recovery(\%) = \left| q_{en} - q_e \right| / q_e \times 100\% \quad (2)$$

where n is the adsorption-desorption cycle.

All experiments were repeated in triplicate and mean value of the results (relative standard error less than 5%) were utilized to data analysis.

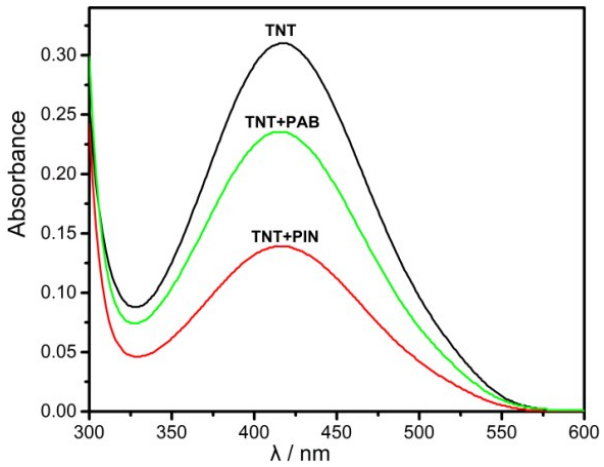

Fig. S7 Characteristic absorbance of (1) TNT solution after adsorption by PAB (2) and PIN (3).

Effects of pH

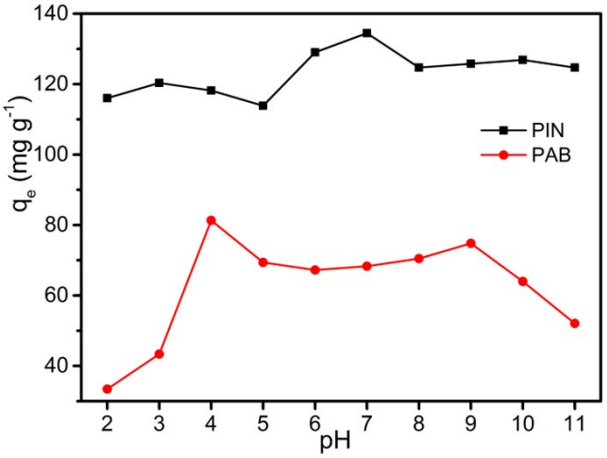

Fig. S8 Effect of solution pH on the TNT adsorption by PIN (black line) and PAB (red line).

Adsorption kinetics results

The pseudo-first-order (PFO), pseudo-second-order (PSO), and intraparticle diffusion

model were employed to evaluate the adsorption kinetic. The corresponding mathematical formulas can be represented as follows: [2,3]

PFO model: $\ln(q_e - q_t) = \ln q_e - k_1 t$ (3)

PSO model: $\frac{t}{q_t} = \frac{1}{k_2 q_e^2} + \frac{t}{q_e}$ (4)

Intraparticle diffusion model: $q_t = k_i t^{1/2} + c$ (5)

where q_t represents the uptake capacity ($mg\ g^{-1}$) at time t, respectively. k_1 (min^{-1}) and k_2 ($g\ mg^{-1}\ min^{-1}$) are the equilibrium rate constants for the PFO and PSO kinetic model, respectively. k_i ($mg\ g^{-1}\ h^{-1/2}$) is intraparticle diffusion rate constant and c ($mg\ g^{-1}$) is the intercept.

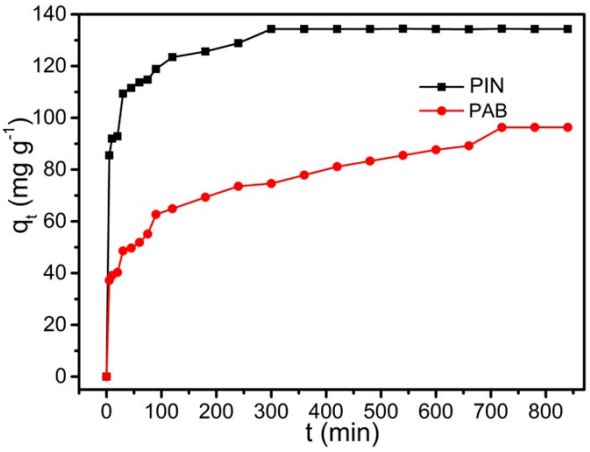

Fig. S9 Adsorption kinetics of PIN (black line) and PAB (red line).

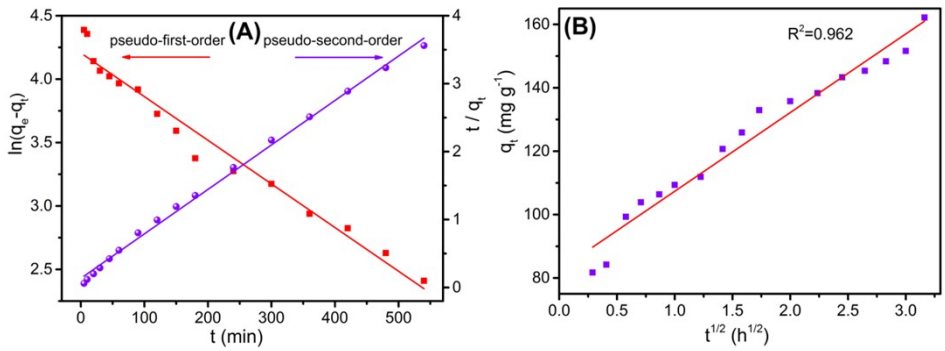

Fig. S10 Adsorption kinetics results of PAIN. (A) PFO and PSO model. (B) Intraparticle diffusion model.

Table S2 Comparison of equilibrium time, q_{max} of various TNT adsorption materials.

Materials	Equilibrium time *(h)*	pH	Temperature *(K)*	q_{max} $(mg\ g^{-1})$
Granular activated carbon[12]	5	3	298	10.65
PA-PSt[13]	3	1	298	11.2
PEI/SiO_2[14]	36	6	298	14.47
PAM/SiO_2[16]	7	6	290	0.873
GO[17]	10		298	62.65
LAC[18]	6	6.7	298	163.79
Modified lignin[29]	24	6-8	298	55.7
Pseudo-graphitic carbon[32]	24	6	293	96.28
PAIN This work	10	7	298	176.7
PIN This work	2	7	298	143.7
PAB This work	12	4	298	110.1

Table S3 The correlated parameters of PFO and PSO kinetic model of TNT adsorption by PAIN.

$q_{e,exp}$	PFO			PSO		
	k_1	$q_{e,cal}$	R^2	k_2	q_e	R^2
162.2	0.00344	67.1	0.970	0.0484	152.9	0.996

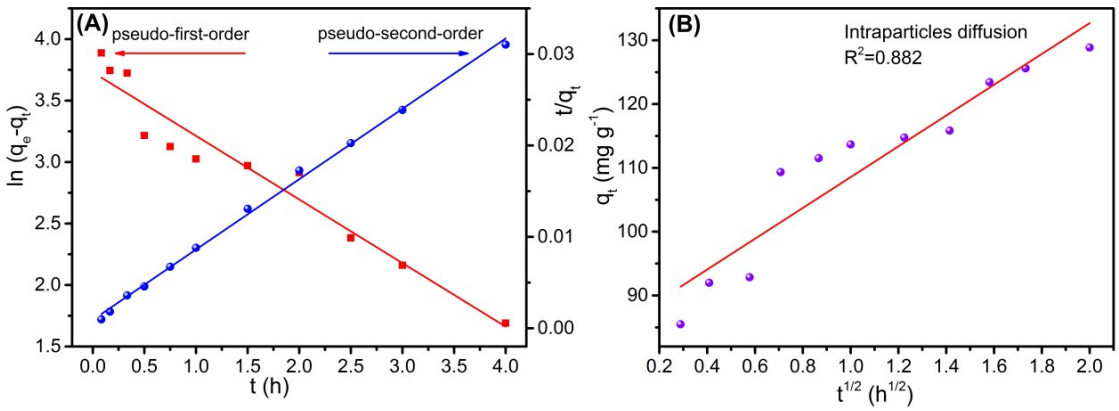

Fig. S11 Adsorption kinetics results of PIN. (A) PFO and PSO model. (B) Intraparticle diffusion model.

Table S4 The correlated parameters of PFO and PSO kinetic model of TNT adsorption by PIN.

$q_{e,exp}$	PFO			PSO		
134.3	k_1	$q_{e,cal}$	R^2	k_2	q_e	R^2
	0.00865	41.4	0.946	0.142	130.2	0.998

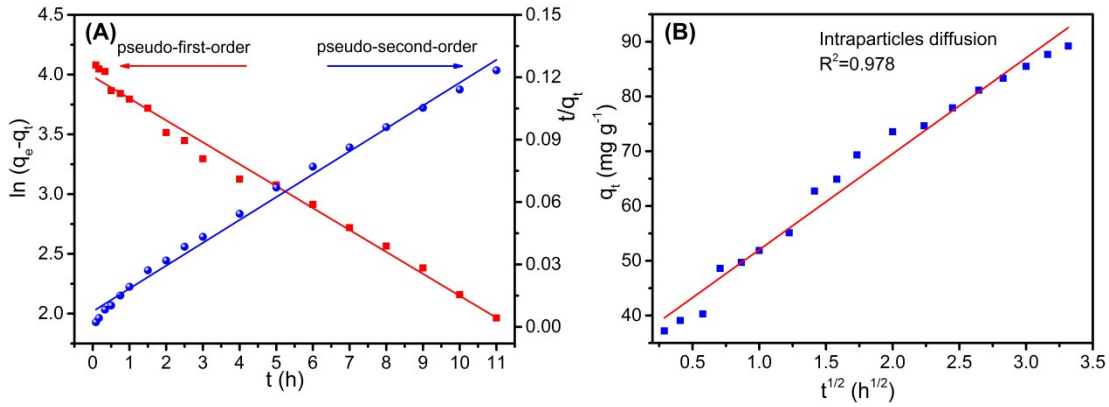

Fig. S12 Adsorption kinetics results of PAB. (A) PFO and PSO model. (B) Intraparticle diffusion model.

Table S5 The correlated parameters of PFO and PSO kinetic model of TNT adsorption by PAB.

$q_{e,exp}$	PFO			PSO		
96.3	k_1	$q_{e,cal}$	R^2	k_2	q_e	R^2
	0.00306	53.7	0.988	0.0246	91.0	0.992

Adsorption isotherm results

The adsorption isotherm data were fitted to both the Freundlich model and the Langmuir model,[4] respectively. The maximum adsorption capacity (q_{max}) was obtained from the Langmuir model.

Freundlich model: $ln\, q_e = ln\, K_F + n\, ln\, c_e$ (6)

Langmuir model: $\frac{c_e}{q_e} = \frac{c_e}{q_{max}} + \frac{1}{q_{max} b}$ (7)

where K_F ($mg\ g^{-1}$) indicated the multilayer adsorption capacity and n an empirical

parameter related to the intensity of adsorption. *b* ($L\ mg^{-1}$) is the Langmuir constant.

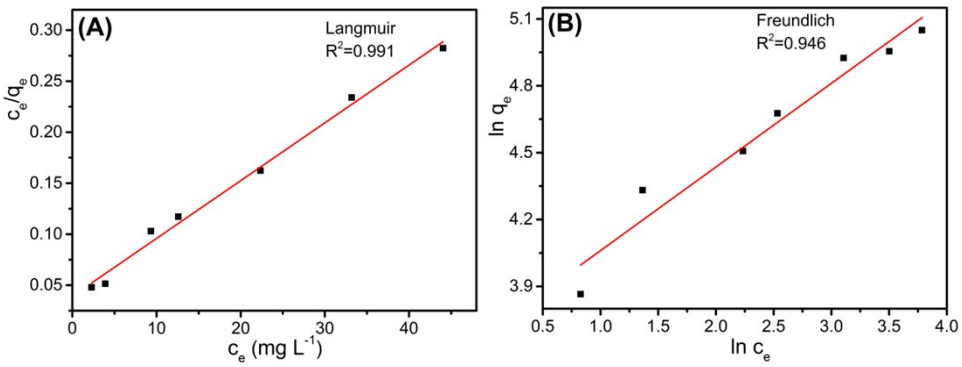

Fig. S13 Fitting results of TNT on PAIN for isotherm models. (A) Langmuir model. (B) Freundlich model.

Table S6 Characteristic parameters obtained by the Freundlich and Langmuir model of PAIN.

Temperature (*K*)	Freundlich constants			Langmuir constants		
	n	K_F	R^2	*b*	q_{max}	R^2
298	0.375	39.9	0.946	0.144	176.7	0.991

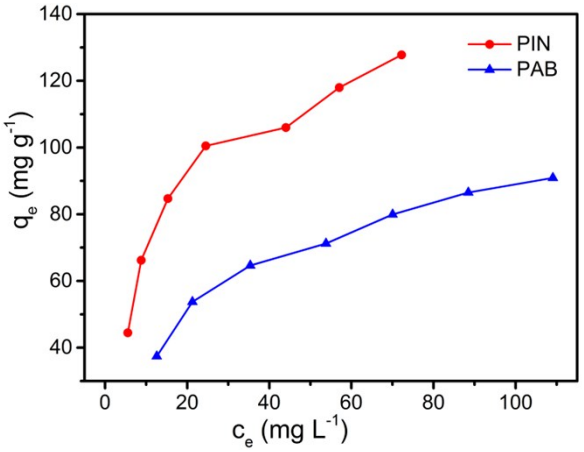

Fig. S14 Adsorption isotherms of PIN (red line) and PAB (blue line).

Table S7 Characteristic parameters obtained by the Freundlich and Langmuir model of PIN.

Temperature (*K*)	Freundlich constants			Langmuir constants		
	n	K_F	R^2	*b*	q_{max}	R^2
298	0.367	27.8	0.911	0.0864	143.7	0.991

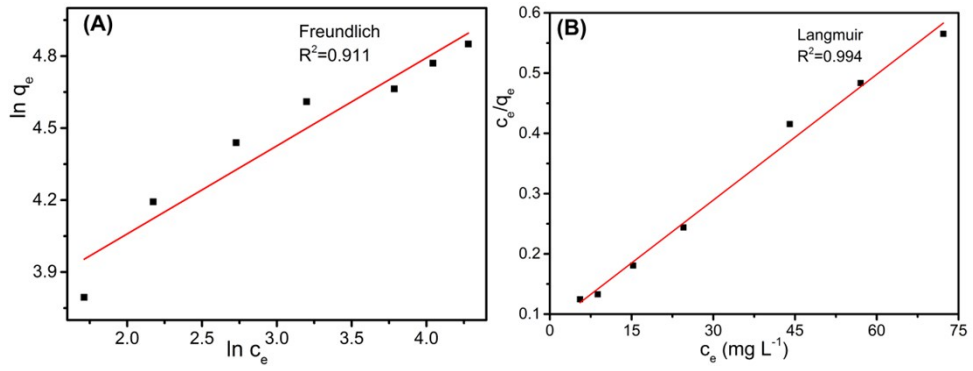

Fig. S15 Fitting results of TNT on PIN for isotherm models. (A) Freundlich model. (B) Langmuir model.

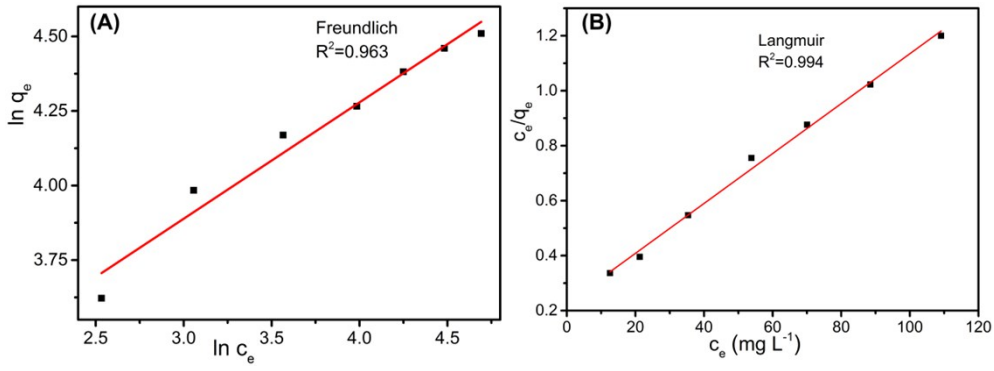

Fig. S16 Fitting results of TNT on PAB for isotherm models. (A) Freundlich model. (B) Langmuir model.

Table S8 Characteristic parameters obtained by the Freundlich and Langmuir model of PAB.

Temperature (*K*)	Freundlich constants			Langmuir constants		
	n	K_F	R^2	*b*	q_{max}	R^2
298	0.390	15.2	0.963	0.0400	110.1	0.994

DFT calculation and results

Density functional theory (DFT) calculations were performed to study the adsorption mechanism. All calculations were accomplished with Materials Studio DMol3 program (Accerlrys. USA).[5-7] For the exchange correlation term of the energy functional, the generalized gradient corrected functional GGA and PW91 functional

as implemented, were used for geometry optimization and energy calculation. The double numerical plus polarization (DNP) basis sets was employed. All the energy values were calculated for 298 K. No restrictions on symmetries were imposed on the initial structures. The frequency analysis was performed on all DFT structures to ensure the absence of imaginary frequency and check on the presence of a true minimum. The computed binding energies for the complexes were defined as,

$$-\Delta E = -\left[E_{A\text{-}B} - \left(E_A + E_B \right) \right] \tag{8}$$

where *A* and *B* are the two interacting molecules.

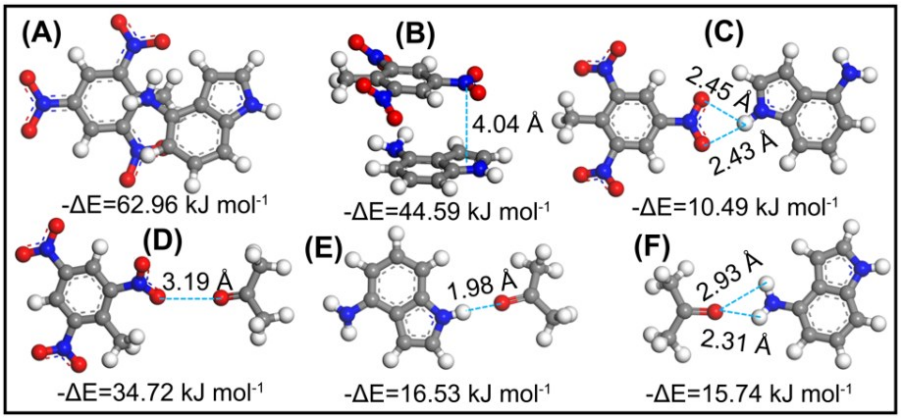

Fig. S17 Fully optimized geometries of model interactions calculated using DFT method. (A) D-A interaction of 4-AIN and TNT. (B) Conformation of face-to-point dipole-π between 4-AIN and TNT. (C) Hydrogen bonding between indole amine with TNT. (D) D-A interaction of acetone and TNT. (E)Hydrogen bonding between indole amine with acetone. (F) Hydrogen bonding between primary amine of 4-AIN with acetone. The white, gray, blue, and red spheres represented hydrogen, carbon, nitrogen, and oxygen atoms, respectively.

Simulation method

In this paper, molecular models were performed on the Amorphous Cell module of the Materials Studio program. The "Compass force field" was used (version 2.8). A single parent chain with 10 repeat units was generated originally. Then, periodic

boundary conditions were imposed and an initial density of 0.86 g cm^{-3} was used to simulate the bulk aggregation structure for model PAIN. Each initial structure was optimized by a molecular mechanics technique. Because this optimized structure might, however, be still in a local energy minimum state, it was relaxed through NPT molecular dynamics (In the canonical ensemble, mole (M), pressure (P), and temperature (T) are conserved), the time evolution of chain conformations up to 1000 ps with time steps of 0.0002 ps at 298 K. The radial distribution function (RDF) is given by the symbol, $g_{AB}(r)$, and is calculated by averaging over the static relationship of every given pair of atoms, *AB*, as follows:

$$g_{AB}(r) = \frac{\langle n_{AB}(r) \rangle}{4\pi r^2 \Delta\rho_{AB}} \tag{9}$$

where *A* and *B* are indole groups and TNT molecules, respectively. $\Delta\rho_{AB}$ is the rate of change of average number density of TNT molecules with the distance from an indole ring. *r* is the distance, and $<n_{AB}>$ is the average number of atom pair between $r+\Delta r$.

References

[1] J. Zhang, X. Lin, X. Luo, C. Zhang and H. Zhu, *Chem. Eng. J.*, 2011, **168**, 1055.

[2] M. A. Shannon, P. W. Bohn, M. Elimelech, J. G. Georgiadis, B. J. Marinas and A. M. Mayes, *Nature,* 2008, **452**, 301.

[3] R. Yu, Y. Shi, D. Yang, Y. Liu, J. Qu and Z. Yu, *ACS Appl. Mater. Inter.,* 2017, **9**, 21809.

[4] Q. Yao, B. Fan, Y. Xiong, C. Jin, Q. Sun and C. Sheng, *Sci. Rep.,* 2017, **7**, 45914.

[5] W. Wang, C. Zhu and Y. Cao, *Int. J. Hydrogen Energ.,* 2010, **35**, 1951.

[6] S. Qu, X. Chen, X. Shao, F. Li, H. Zhang, H. Wang, P. Zhang, Z. Yu, K. Wu, Y. Wang and M. Li, *J. Mater. Chem.,* 2008, **18**, 3854.

[7] R. Lü, J. Lin and Z. Qu, *Comput. Theor. Chem.,* 2012, **1002**, 49.